

Incorporation of Reversible Electroporation Into Electrolysis Accelerates Apoptosis for Rat Liver Tissue

Technology in Cancer Research & Treatment
Volume 19: 1-8
© The Author(s) 2020
Article reuse guidelines:
sagepub.com/journals-permissions
DOI: 10.1177/1533033820948051
journals.sagepub.com/home/tct


Hong Bae Kim, PhD¹ and Jong Hoon Chung, PhD^{1,2}

Abstract

Tissue electrolysis is an alternative modality that uses a low intensity direct electric current passing through at least 2 electrodes within the tissue and resulting electrochemical products including chlorine and hydrogen. These products induce changes in pH around electrodes and cause dehydration resulting from electroosmotic pressure, leading to changes in microenvironment and thus metabolism of the tissues, yielding apoptosis. The procedure requires adequate time for electrochemical reactions to yield products sufficient to induce apoptosis of the tissues. Incorporation of electroporation into electrolysis can decrease the treatment time and enhance the efficiency of electrolytic ablation. Electroporation causes permeabilization in the cell membrane allowing the efflux of potassium ions and extension of the electrochemical area, facilitating the electrolysis process. However, little is known about the combined effects on apoptosis in liver ablation. In this study, we performed an immunohistochemical evaluation of apoptosis for the incorporation of electroporation into electrolysis in liver tissues. To do so, the study was performed with microelectrodes for fixed treatment time while the applied voltage varied to increase the applied total energy for electrolysis. The apoptotic rate for electrolytic ablation increased with enhanced applied energy. The apoptotic rate was 4.31 ± 1.73 times that of control in the synergistic combination compared to 1.49 ± 0.33 times that of the control in electrolytic ablation alone. Additionally, tissue structure was better preserved in synergistic combination ablation compared to electrolysis with an increment of 3.8 mA. Thus, synergistic ablation may accelerate apoptosis and be a promising modality for the treatment of liver tumors.

Keywords

electroporation, electrolysis, microelectrode, apoptosis, synergistic effect

Abbreviations

TUNEL, terminal deoxynucleotidyl transferase dUTP nick end labeling; H&E, hematoxylin and eosin

Received: January 28, 2020; Revised: June 20, 2020; Accepted: July 9, 2020.

Introduction

Minimally invasive ablation has received increasing attention in modern medicine and is generally divided into 2 types, radiofrequency ablation and microwave ablation,¹ both of which use electromagnetic waves as the energy source. The electromagnetic wave is defined by its wavelength or frequency of oscillation.² The effects of electromagnetic radiation on biological organisms depend upon both the power and frequency of the radiation.³ The radiation primarily causes heating from the combined energy transfer of many photons. The heating effect on biological tissues causes cell death due to coagulation necrosis, in which tissues are converted into a dry homogeneous eosinophilic mass as a result of protein

coagulation.^{4,5} This induces an inflammatory response. To remove the dead cells by phagocytosis, the response attracts leukocytes and nearby phagocytes.⁶ The leukocytes release

¹ Department of Biosystems & Biomaterials Science and Engineering, Seoul National University, Seoul, Republic of Korea

² Research Institute for Agriculture and Life Sciences, Seoul National University, Seoul, Republic of Korea

Corresponding Author:

Jong Hoon Chung, Department of Biosystems & Biomaterials Science and Engineering and Research Institute for Agriculture and Life Sciences, Seoul National University, Seoul 08826, Republic of Korea.
Email: jchung@snu.ac.kr



substances that damage microbes, creating collateral damage to the surrounding tissues and further inhibiting the healing process.⁶ Such necrosis of tumor tissues increases post-treatment recovery time. Recently, non-thermal ablation has been a focus of research. Electrochemical treatment via electrolysis as a non-thermal biophysical mechanism involves the application of low-voltage direct current to the tissue.⁷ Direct current is the unidirectional flow of an electric charge without frequency and produces various electrochemical reactions resulting from electrical charges passing through tissues, resulting in the creation of electrolysis products. These products change the local pH, which causes cell death. This process requires sufficient time for the electrochemical reactions and for electrolysis products to diffuse into tissues.^{7,8} Due to the long reaction time, interest in clinical applications of electrolysis has waned.

However, the introduction of electroporation into electrolysis has revived attention for clinical application.⁹⁻¹³ Permeabilization of the cell membrane by electroporation sensitizes the cells to the evolutions of electrolysis.¹⁴ Typically, electroporation involves an application of a direct current pulse below the electric field threshold of the target tissue to produce reversible electroporation that reseals pores in the membrane. As a non-thermal modality, reversible electroporation causes less muscle contraction than irreversible electroporation, which uses a stronger electric field to prevent resealing of pores in the membrane. Incorporating reversible electroporation into electrolysis has the advantages of enhancing the efficiency of electrolytic ablation while simultaneously mitigating muscle contractions. The synergistic combination makes the cell more susceptible to lesser amounts of electrolysis products.¹⁵ Electrolysis plays a key role in their combination and requires optimization of initial voltage and total applied electrical charge based on electrode configurations to maximize their synergistic performance.⁹⁻¹³ Several previous studies have performed synergistic ablation histologically, focusing on electrical parameters and electrode geometric configurations,¹⁴⁻¹⁷ yet it remains challenging to achieve. In this study, we performed an immunohistochemical evaluation of apoptosis to quantify the effects of variations in electrical energy used in electrolysis and the synergistic coupling of electrolysis with electroporation using microscale electrodes. Additionally, the advantages of synergistic ablation have been addressed at the cellular level.

Materials and Methods

Simulation of Applied Electric Fields

The Laplace equation governs the external applied electric field strength between electrodes. By solving the equation, we obtain a steady-state electric field distribution as follows:

$$\nabla^2 \varnothing = 0 \quad (1)$$

where \varnothing is the externally applied electric potential, assuming that an electrode length is greater than the distance between the electrodes. The tissue surface effect is neglected.¹⁸ The electric

field strength is given like a gradient of the external electric potential:

$$E = \nabla \varnothing \quad (2)$$

The boundary condition of the applied tissue is defined as either $\varnothing = V_0$ or 0. The resting boundaries were electrically postulated as insulating ($\frac{d\varnothing}{dn} = 0$). The electric field was calculated using Epo codeTM developed with the open-source software OpenFOAM (The Standard Co. Ltd., Korea).

Experimental Animals and Procedures for Electrical Ablation

A protocol for this experiment obtained approval from the Animal Care and Use Committee of Seoul National University (SNU-120409-3). All experimental procedures were conducted in accordance with approved institutional guidelines. Eight-week-old male rats of Sprague Dawley that ranged in weight from 260 to 300 g were maintained in an animal cage and were allowed to adapt for 2 weeks to give relaxation. All procedures were performed under anesthetization using 10 mg/kg Zoletil via intraperitoneal injection (Virbac, France). The animals were randomly divided into 9 groups, namely, control, 1.5V8 s, 3V8 s, 3V60 s, 15V8 s, 15V60 s, 20V8 s, 1000V8P, and 15V8s-1000V8P groups (n = 3 animals per group). After sterilizing a shaved site, an abdominal incision was made 15 mm in length and then the entire liver was exposed. The electrode was made using previously approved methods¹⁹ with stainless steel wires 100 μ m in diameter, 5 mm long, with center-to-center distance averaging 1 ± 0.16 mm and was carefully penetrated perpendicular to the liver surface to a depth of 5 mm (Figure 1Aa). To avoid corrosion from the electrochemical reaction, the electrode was used only once for each set of experimental conditions. Ablation was incurred on each of the 3 lobes of the liver.

For electrolytic ablation, direct current was applied for 8 s at a time with voltages of 1.5, 3.0, 15.0, and 20.0 V to generate electric field strengths of 10, 20, 100, and 130 V/cm, respectively, at the midpoint between electrodes. To ascertain diffusion of electrolysis products into tissues, 3 and 15 V of direct current were applied for 60 sec. For electroporation ablation, eight 150 V square pulses of 100 μ s length were applied at a frequency of 1 Hz to achieve 1,000 V/cm of electric field strength at the midpoint between electrodes. The pulses occurred at an interval of 1 s to avoid the effects of thermal energy on tissues as shown in a previous study.¹⁹ For the synergistic effect of electroporation and electrolysis on tissue ablation, 8 square pulses of 1,000 V/cm electric field strength were applied, and then 100 V/cm direct current was immediately applied for 8 s. A direct current power supply (PL-3003D, Protek, Korea) and a pulse generator (EpoTM, The Standard, Co. Ltd., Korea) were used. For the pulse generator, 1,000 Ω -cement resistor of 5 watts was employed parallel to the load to ensure proper square pulse shape and to inhibit delivery of pulses to an open circuit. In the synergistic case, an automatically activated relay module (G2R-2 DC 12 V, OMRON,

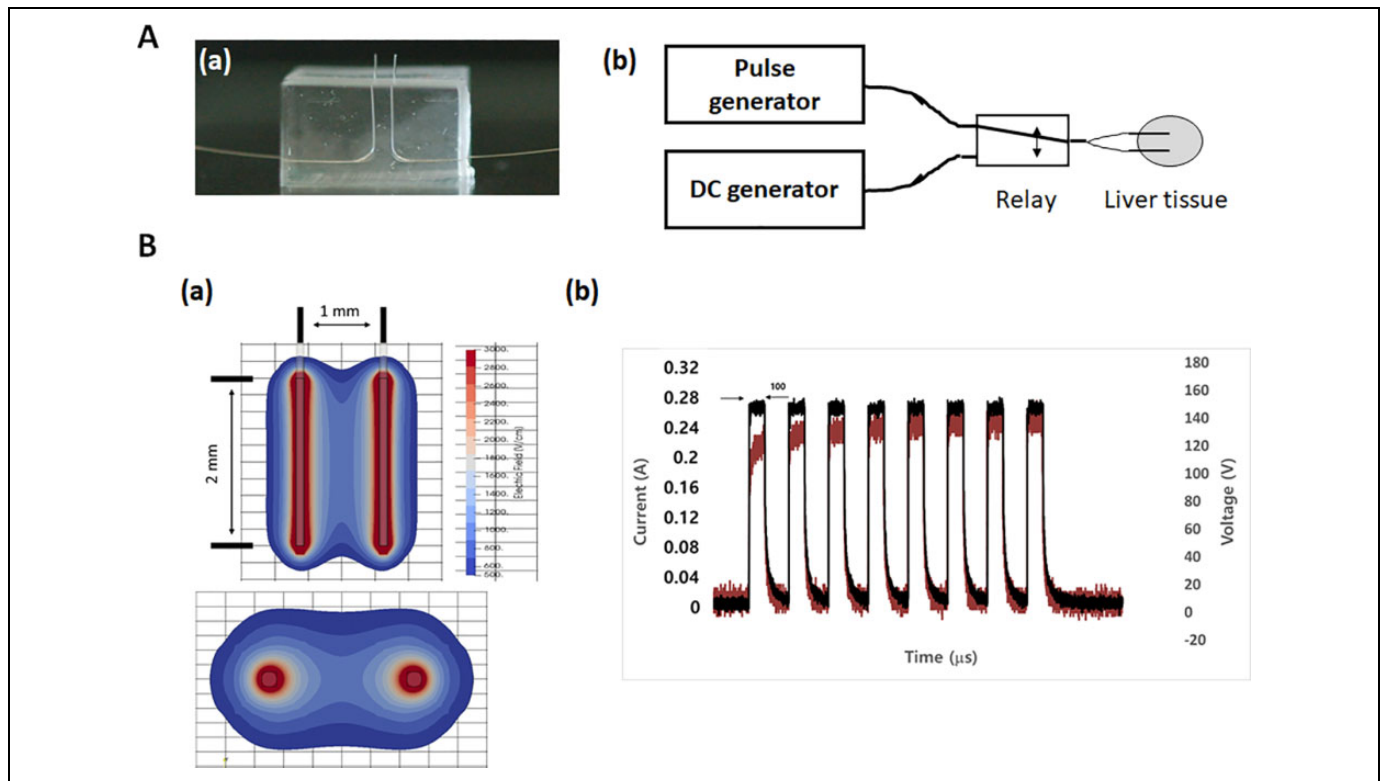


Figure 1. Experimental set-up for electroporation. (A). The stainless steel needle used for electroporation was 100 μm in diameter with 5 mm of exposure length and positioned with 1 mm average center-to-center distance (a) and configuration of the pulse generator and direct current generator (b). (B). Representative electric field distribution for 1000 V/cm applied at the midpoint between electrodes (a) and waveform of eight 150 V square pulses of 100 μs length and resulting current (b).

Japan) was employed to stimulate direct current after electroporation without a time delay (Figure 1Ab). To measure the current passing through tissues, a multimeter (Protek 608, Protek, Korea) was linked in series to an electrode through the DC power supply. Additionally, a current probe (TCPA300, Tektronix, USA) that connected to a digital oscilloscope (TDA3044B, Tektronix, USA) was clamped to an electric wire from the pulse generator. To compare electrolytic ablation with electroporation, the applied electrical energy was calculated as follows²⁰:

$$\text{Electrical Energy} = E^2 T_p N \quad (3)$$

where E is the external applied electric field strength, T_p is the pulse width, and N is the number of pulses. Using this equation, we calculated the values for applied electrical energy as in Table 1. After completing the stimulation, each ablation was marked with tissue marking dye (MDT100, Sigma-Aldrich, USA). After anesthetizing, at 10 hours¹⁹ the ablated and control tissues were harvested and then the animals were euthanized.

Histological Analysis

After fixing the tissues in 10% buffered formalin (vol/vol), paraffin sections of 10 μm thickness were cut in a cross-sectional direction to the electrode at 1 mm from the tissue surface and mounted onto microscope slides. To assess the

degree of necrosis, sectioned tissue was stained with hematoxylin and eosin (H&E), and the following section with a terminal deoxynucleotidyl transferase dUTP nick end labeling (TUNEL; S7100, Millipore, CA) assay kit for assessment of apoptosis. The slides were put under microscope (Olympus BX-51) and images were taken using a digital system (Image-Pro plus 4.5). Quantifying the apoptotic area was carried out according to a previous area-based evaluation method.^{19,21,22} In brief, the 4X-scaled TUNEL assay images were converted into gray-scale images. The images adjusted to be at least 25% darker than non-stained normal tissue. The darkened area was calculated via ImageJ.

Statistical Analysis

The data present the mean with standard deviation and have been statistically evaluated by unpaired Student's t -test (2-tailed) using Microsoft Excel, where *, **, and *** indicate P -values < 0.05 , < 0.01 , and < 0.001 , respectively, compared to the control value, and # represents a P -value compared with the other group.

Results

A representative electric field distribution was simulated between the electrodes for 1,000 V/cm of electroporation at

Table 1. Relevant Parameters for the Present Study.

Items	Applied voltage (V)	Cumulative time (s)	Electric field (V/m)	Electric energy (*10 ⁶ V ² ·s/m ²)	Current (A)
1.5V8s	1.5	8	1,000	8	1.00E-11
3V8s	3	8	2,000	32	2.33E-05
3V60s	3	60	2,000	240	2.33E-05
15V8s	15	8	10,000	800	4.00E-03
15V60s	15	60	10,000	6,000	4.00E-03
20V8s	20	8	13,333	1,422	1.12E-02
1000V8P	150	0.0008	100,000	8	2.56E-01 _{peak}
15V8s1000V8P				808	1.50E-02

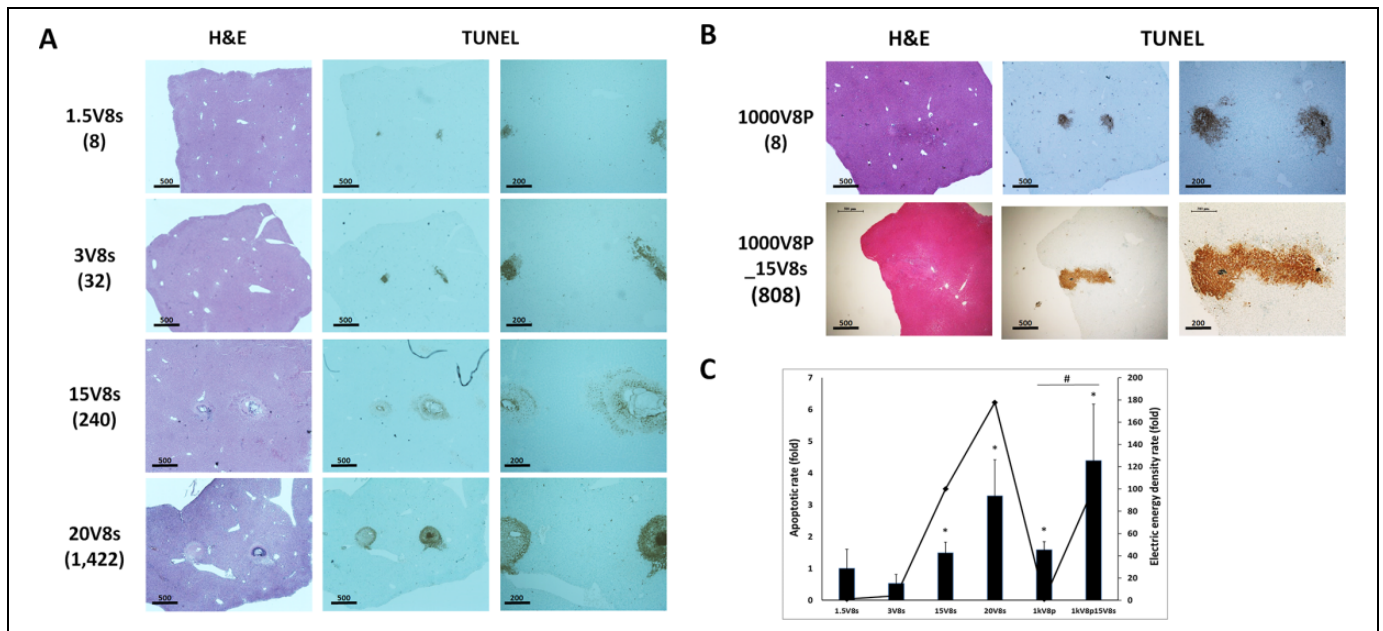


Figure 2. Ablation induced with direct current, electroporation, and synergistic stimulation assessed by H&E staining and TUNEL assay. (A) The applied voltages of the direct current were 1.5, 3, 15, and 20 V for 8 sec. (B) Electroporation used an electric field strength of 1,000 V/cm generated by 8 pulses of width of 100 μ s and interval of 100 μ s. The synergistic stimulation consisted of electroporation (1,000 V/cm) and then electrolysis (15 V for 8 sec). The value in brackets indicates the applied electrical energy for comparison ($\times 10^6$ V²·s/m²). Scale bar is 500 μ m. Magnified images of TUNEL assay have 200 μ m scale bar. (C) The apoptotic rate caused by direct current, electroporation and synergistic stimulation. Data are the mean \pm SD ($n = 3$). P -value determined by a 2-tailed t -test.

the midpoint between the electrodes. The distribution was even, neglecting fields at the edges of electrodes (Figure 1Ba). Based on this simulation, the waveforms of the applied voltages and resulting current are shown, which was taken in a single mode under a setting 100 μ s in length and a 100 μ s interval (Figure 1Bb). All electroporation in this study was conducted under such conditions. For electrical ablation, electrical stimulation was first performed for electrolytic ablation on rat liver tissue using direct current. The ablation area of the positive electrode was wider than that of the negative one. The apoptotic rate generally increased with direct current energy (Figure 2). The quantitative apoptotic rate for 3V8 s, 15V8 s, and 20V8 s was 0.53 ± 0.28 , 1.49 ± 0.33 ($P < 0.05$), and 3.28 ± 1.13 ($P < 0.05$) times that of 1.5V8 s, respectively. The apoptotic rate was also compared with that of electroporation. The rate of electroporation was 1.58 ± 0.25 ($P < 0.05$)

times that of 1.5V8 s, even though the applied electrical energy was the same as that of 1.5V8 s. The synergistic effect of electroporation and electrolysis (15V8s-1000V8P) appeared to be 4.31 ± 1.73 ($P < 0.05$) times that of 1.5V8 s, although the applied electrical energy was only 8 times higher than that of 1.5V8 s (Figure 2).

Changes in tissues were dependent on electrical ablation. Tissue subjected to electrolytic ablation showed almost complete destruction around an electrode, while electroporation left some collagen fibers in the tissue. Tissue treated by synergistic ablation exhibited an appearance similar to that of electroporation ablation. Tissues treated with electrolytic ablation did not show nuclear contours, although tissues subjected to electroporation and synergistic ablation showed precise contours of nuclei, in conjunction with cell death seen as pyknosis and karyorrhexis (Figure 3).

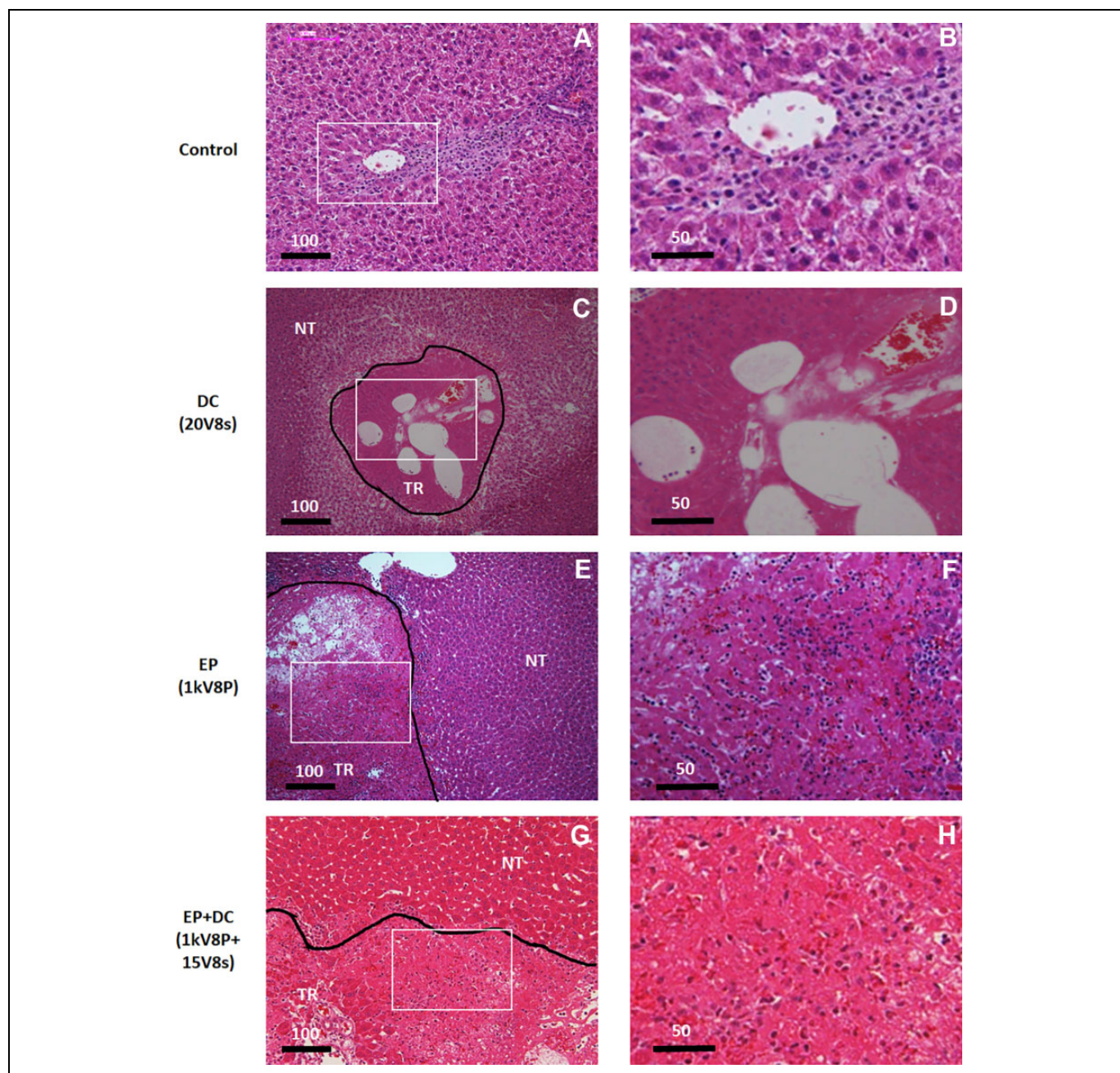


Figure 3. Histological analysis (H&E staining) of liver sections obtained from untreated rats (control), direct current (20V8 s), electroporation (1000V8P), and the synergistic treatment (1000V8P+15V8 s). NT denotes an untreated region; TR, a treated area around the cathodic electrode. Scale bars, 100 μm , and 50 μm .

Discussion

In the current study, an electrochemical system composed of 2 electrodes is separated by 2-phase of electrolysis, here consisting of various ion-containing biological tissues. The potential difference between electrodes causes charge transport across the electrode/electrolyte interface, which produces a current. The current between electrodes causes chemical reactions and production of electrical energy. The electrochemical reactions include decomposition of water to produce oxygen and oxidation of chloride to produce chlorine at the anode. At the

cathode, evolution of hydrogen leads to production of hydroxide ions.²³ Chloride ions accumulate around the anode and react with H^+ to yield HCl, producing cytotoxicity. Additionally, the chlorine produces an acid toxic to local tissue, while hydrogen produces local cavitation.^{24,25} During these reactions, the reactants produce changes in the pH of tissue around the electrodes, with lower values like pH 1.0 in the tissues around the anode and as high as pH 13.0 near the cathode.²⁶ During these electrochemical reactions, cytotoxic effects spread into the surrounding tissues. Moreover, electro-osmotic

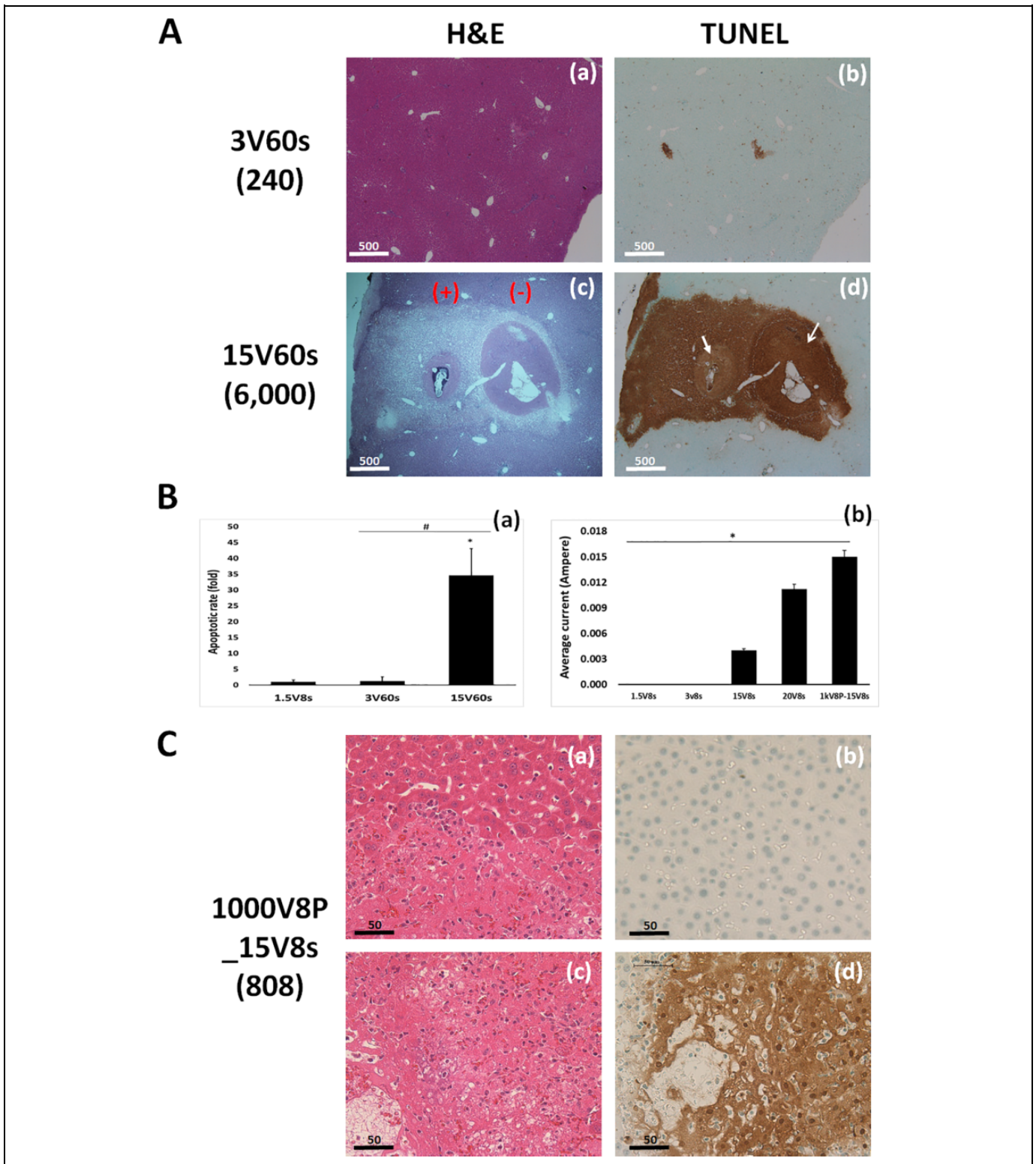


Figure 4. The comparison of electrochemical reactions from low and high direct current energy and the synergistic stimulation. (A) H&E staining and TUNEL assay of liver sections from rats subjected to voltages of 3 and 15 V of direct current for 60 sec. Arrows (the anode and the cathode) indicate thermal injury from an electrochemical reaction. Scale bar, 500 μm . (B) The apoptotic rate caused by direct current (a). The average current passing through tissues between electrodes for electrolysis, electroporation, and their synergistic combination (b). Data are mean \pm SD ($n = 3$). P -value determined by a 2-tailed t -test. (C) Tissue preservation under 8 pulses 1000 V/cm and then 15 V for 8 sec of synergistic stimulation. The boundary of non-ablated and ablated area (a), not-stained TUNEL (b), ablated area (c), and stained TUNEL (d). The value in brackets indicates the applied electrical energy for comparison ($\times 10^6 \text{ V}^2 \cdot \text{s}/\text{m}^2$). Scale bar, 50 μm .

forces caused by the external applied electric field drive the migration of water toward the cathode in the same direction as the electric field, magnifying the physiological effects around the electrodes.²⁷ Such a cytotoxic environment causes cell death through apoptosis in proportion to the applied electrical energy. The present study supports these findings. Increasing the applied voltage produced increased levels of electrochemical reactants, resulting in a widened ablation area, as shown in Figures 2 and 3. To clarify these electrochemical effects, the applied energy was increased in 2 ways; increasing either the applied voltage or the time according to equation (3). While tissue under 3V60 s showed mild damage, tissue subjected to 15V60 s showed severe apoptosis around the electrodes, as well as farther away, due to diffusion of electrochemical products (Figure 4A). The resulting apoptotic rate relative to that of 1.5V8 s was higher in tissue subjected to 15V60 s (1.21 ± 1.36 fold for 3V60 s (NS), 34.57 ± 8.46 fold for 15V60 s; $P < 0.05$ compared to 1.5V8 s; $P < 0.05$ compared to 3V60 s) (Figure 4Ba). Also, the result of 15V60 s showed intense apoptosis resulting from diffusion of cytotoxic reactants into tissues surrounding the electrodes. That may presumably be in addition to a thermodynamic result of the electrochemical reaction,²⁵ including the electrical corrosion reactions of the electrodes themselves.

Electroporation, by contrast, hardly produce electrochemical reactants cytotoxic to tissues due to short enough pulses.²⁸ Despite the lower applied electric energy of reversible electroporation compared to electrolysis, more intensive apoptosis was produced with reversible electroporation than with electrolysis. This was a direct result of the different mechanisms used to induce apoptosis. In contrast to electrolysis, electroporation involves the application of short high voltage pulses to cells or tissues. The electric fields increase the transmembrane potential, charging the membrane like a capacitor by moving ions from the surrounding solution. The increased transmembrane potential induces the formation of pores, either reversibly for permeabilization or irreversibly for ablation of tumor cells.²⁹ Additionally, electroporation generates a response in objects with electro-potential and preserves the extracellular matrix and nerve and blood systems. In the present study, the electroporation technique revealed preservation of tissues (Figure 3).

Furthermore, synergistic ablation takes advantage of both electroporation and electrolysis resulting from the direct current. Many pores generated by electroporation allow efflux of intracellular potassium ions. The direct current causes strong electrochemical reactions around the electrodes due to a number of ions from the efflux. Thus, synergistic ablation enhances the efficacy of the direct current. This study reveals the enhanced effect of synergistic ablation relative to that of direct current or electroporation alone (Figure 2). The amount of current passing through tissues between the electrodes reflected the synergistic ablation. For electrolysis, voltages of 1.5, 3, 15, and 20 V induced currents of 1.0 pA, 23.3 μ A, 4.0 mA, and 11.2 mA, respectively (Table 1). The synergistic combination induced a current of 15.0 mA, a 3.75-fold increase relative to that of 15V8 s electrolysis alone (Figure 4Bb). Moreover,

improved preservation of tissue was observed in synergistic ablation as compared to only electrolysis (Figure 4C).

In summary, electrolytic ablation is a chemical reaction process. Electrolysis products diffuse out from ambient electrodes. Thus the disadvantage of a long time required for diffusion of the products, despite the high efficiency of the ablation. However, coupling electrolysis with electroporation can accelerate the ablation. The present study shows the effects of synergistic ablation on rat-liver tissue. These results may be used as a basis to treat liver tumors by means of synergistic ablation using electrolysis and electroporation.

Acknowledgments

The authors acknowledge Choi, YS. for electrode support of the study.

Declaration of Conflicting Interests

The author(s) declared no potential conflicts of interest with respect to the research, authorship, and/or publication of this article.

Funding

The author(s) disclosed receipt of the following financial support for the research, authorship, and/or publication of this article: The authors received financial support by the National Research Foundation of Korea (2017M3A9B403364) for the research, authorship, and/or publication of this article.

References

1. Antonio F, Marianna DM, Nicola M. Microwave ablation versus radiofrequency ablation for the treatment of hepatocellular carcinoma: a systematic review and meta-analysis. *Int J Hyperthermia*. 2016;32(3):339-344.
2. Kleidon A. Energy balance. In: Fath BD, ed. *Encyclopedia Ecology*. Elsevier; 2008:1276-1289.
3. Daniel A, Trevor M. Radiation. *Unraveling Environmental Disasters*. 2003;299-320.
4. Sun Y, Wang Y, Ni X, Gao Y, Shao Q, Liu L. Comparison of ablation zone between 915- and 2450-MHz cooled-shaft microwave antenna: results in in vivo porcine livers. *AJR Am J Roentgenol*. 2009;192(2):511-514.
5. Xu Y, Shen Q, Wang N, et al. Microwave ablation is as effective as radiofrequency ablation for very-early-stage hepatocellular carcinoma. *Chin J Cancer*. 2017;36:14.
6. Rock KL, Kono H. The inflammatory response to cell death. *Annu Rev Pathol*. 2008;3:99-126.
7. Olaiza N, Maglietta F, Suáreza C, et al. Electrochemical treatment of tumors using a one-probe two-electrode device. *Electrochimica Acta*. 2010;55:6010-6014.
8. Vijn AK. Electrochemical field effects in biological materials: electro-osmotic dewatering of cancerous tissue as the mechanistic proposal for the electrochemical treatment of tumors. *J Mater Sci Mater Med*. 1999;10:419-423.
9. Phillips M, Rubinsky L, Meir A, Raju N, Rubinsky B. Combining electrolysis and electroporation for tissue ablation. *Technol Cancer Res Treat*. 2015;14:395-410.

10. Stehling MK, Guenther E, Mikus P, Klein N, Rubinsky L, Rubinsky B. Synergistic combination of electrolysis and electroporation for tissue ablation. *PLoS One*. 2016;11:e0148317.
11. Rubinsky L, Guenther E, Mikus P, Stehling M, Rubinsky B. Electrolytic effects during tissue ablation by electroporation. *Technol Cancer Res Treat*. 2016;15:NP95-NP103.
12. Klein N, Mercadal B, Stehling M, Ivorra A. In vitro study on the mechanisms of action of electrolytic electroporation (E2). *Bioelectrochemistry*. 2020;133:107482.
13. Guenther E, Klein N, Mikus P, et al. Toward a clinical real time tissue ablation technology: combining electroporation and electrolysis (E2). *PeerJ*. 2020;8:e7985.
14. Klein N, Guenther E, Botea F, et al. The combination of electroporation and electrolysis (E2) employing different electrode arrays for ablation of large tissue volumes. *PLoS One*. 2019;14:e0221393.
15. Phillips M, Raju N, Rubinsky L, Rubinsky B. Modulating electrolytic tissue ablation with reversible electroporation pulses. *Technology*. 2015; 3(1):45-53.
16. Phillips M, Krishnan H, Raju N, Rubinsky B. Tissue ablation by a synergistic combination of electroporation and electrolysis delivered by a single pulse. *Ann Biomed Eng*. 2016;44(10):3144-3154.
17. Klein N, Guenther E, Mikus P, Stehling MK, Rubinsky B. Single exponential decay waveform; a synergistic combination of electroporation and electrolysis (E2) for tissue ablation. *PeerJ*. 2017; 5:e3190.
18. Sung CK, Kim HB, Jung JH, et al. Histological and mathematical analysis of the irreversibly electroporated liver tissue. *Technol Cancer Res Treat*. 2017;16(4):488-496.
19. Choi YS, Hong-Bae K, Chung J, Hyung-Sik K, Jeong-Han Y, Je-Kyun P. Preclinical analysis of irreversible electroporation on rat liver tissues using a microfabricated electroporator. *Tissue Eng Part C Methods*. 2010;16(6):1245-1253.
20. Sano MB, Arena CB, Bittleman KR, et al. Bursts of bipolar microsecond pulses inhibit tumor growth. *Sci Rep*. 2015;5:14999.
21. Leu JI, Crissey MAS, Taub R. Massive hepatic apoptosis associated with TGF- β 1 activation after fas ligand treatment of IGF binding protein-1 deficient mice. *J Clin Invest*. 2003;111(1):129-139.
22. Liu L, Cao Y, Chen C, et al. Sorafenib blocks the RAF/MEK/ERK pathway, inhibits tumor angiogenesis, and induces tumor cell apoptosis in hepatocellular carcinoma model PLC/PRF/5. *Cancer Res*. 2006;66(24):11851.
23. Gu YH, Yamashita T, Inoue T, Song JH, Kang KM. Cellular and molecular level mechanisms against electrochemical cancer therapy. *J Pathog*. 2019;3431674.
24. Kim HB, Ahn S, Jang HJ, Sim SB, Kim KW. Evaluation of corrosion behaviors and surface profiles of platinum-coated electrodes by electrochemistry and complementary microscopy: biomedical implications for anticancer therapy. *Micron*. 2007;38(6):747-753.
25. Holandino C, Veiga VF, Capella MM, Menezes S, Alviano CS. Damage induction by direct electric current in tumoural target cells. *Indian J Exp Biol*. 2000;38:554-558.
26. von Euler H, Nilsson E, Olsson JM, Lagerstedt AS. Electrochemical treatment (EChT) effects in rat mammary and liver tissue. In vivo optimizing of a dose-planning model for EChT of tumours. *Bioelectrochemistry*. 2001;54(2):117-124.
27. Ciria HM, González MM, Zamora LO, et al. Antitumor effects of electrochemical treatment. *Chin J Cancer Res*. 2013;25(2):223-234.
28. Morren J, Roodenburg B, de Haan SWH. Electrochemical reactions and electrode corrosion in pulsed electric field (PEF) treatment chamber. *Innovative Food Sci Emerg Technol*. 2003;4(3):285-295.
29. Kotnik T, Frey W, Sack M, Meglič SH, Peterka M, Miklavčič M. Electroporation-based applications in biotechnology. *Trends Biotechnol*. 2015;33(8):480-488.